BMC Physiology

BioMed Central

Research article

Atypical properties of a conventional calcium channel β subunit from the platyhelminth *Schistosoma mansoni*

Vicenta Salvador-Recatalà*[1,3], Toni Schneider[2] and Robert M Greenberg[1,3]

Address: [1]Marine Biological Laboratory 7 MBL Street Woods, Hole, MA 02543, USA, [2]Institute for Neurophysiology & Center for Molecular Medicine Cologne (CMMC) Robert-Koch-Str. 39 D-50931 Köln, Germany and [3]Department of Pathobiology, School of Veterinary Medicine, University of Pennsylvania, 3800 Spruce Street, Philadelphia, PA 19104, USA

Email: Vicenta Salvador-Recatalà* - vsalvador@mbl.edu; Toni Schneider - toni.schneider@uni-koeln.de; Robert M Greenberg - rgree@vet.upenn.edu

* Corresponding author

Abstract

Background: The function of voltage-gated calcium (Ca_v) channels greatly depends on coupling to cytoplasmic accessory β subunits, which not only promote surface expression, but also modulate gating and kinetic properties of the α_1 subunit. Schistosomes, parasitic platyhelminths that cause schistosomiasis, express two β subunit subtypes: a structurally conventional β subunit and a variant β subunit with unusual functional properties. We have previously characterized the functional properties of the variant $Ca_v\beta$ subunit. Here, we focus on the modulatory phenotype of the conventional $Ca_v\beta$ subunit ($SmCa_v\beta$) using the human $Ca_v2.3$ channel as the substrate for $SmCa_v\beta$ and the whole-cell patch-clamp technique.

Results: The conventional *Schistosoma mansoni* $Ca_v\beta$ subunit markedly increases $Ca_v2.3$ currents, slows macroscopic inactivation and shifts steady state inactivation in the hyperpolarizing direction. However, currents produced by $Ca_v2.3$ in the presence of $SmCa_v\beta$ run-down to approximately 75% of their initial amplitudes within two minutes of establishing the whole-cell configuration. This suppressive effect was independent of Ca^{2+}, but dependent on intracellular Mg^{2+}-ATP. Additional experiments revealed that $SmCa_v\beta$ lends the $Ca_v2.3/SmCa_v\beta$ complex sensitivity to Na^+ ions. A mutant version of the $Ca_v\beta$ subunit lacking the first forty-six amino acids, including a string of twenty-two acidic residues, no longer conferred sensitivity to intracellular Mg^{2+}-ATP and Na^+ ions, while continuing to show wild type modulation of current amplitude and inactivation of $Ca_v2.3$.

Conclusion: The data presented in this article provide insights into novel mechanisms employed by platyhelminth $Ca_v\beta$ subunits to modulate voltage-gated Ca^{2+} currents that indicate interactions between the Ca^{2+} channel complex and chelated forms of ATP as well as Na^+ ions. These results have potentially important implications for understanding previously unknown mechanisms by which platyhelminths and perhaps other organisms modulate Ca^{2+} currents in excitable cells.

Background

Voltage-gated calcium (Ca_v) channels couple membrane depolarisation to the entry of Ca^{2+} that, in turn, is funda-

mental in a variety of cellular events such as contraction [1,2], changes in gene expression [3] and neurotransmitter release [4,5]. Ca_v channels belong to the super-family

of voltage-gated ion channels that also include sodium channels and potassium channels [6], and can be broadly classified into high-voltage activated (HVA) and low-voltage activated (LVA) classes. HVA Ca_v channels are heteromeric protein complexes composed of a pore-forming α_1 subunit and auxiliary β and $\alpha_2\delta$ subunits [7]. In addition to promoting surface expression of the $Ca_v\alpha_1$ subunit, $Ca_v\beta$ subunits modulate the kinetics of activation and inactivation, gating [8-10] and the rate of recovery from inactivation [11,12].

Schistosomes are parasitic trematode flatworms that cause schistosomiasis, a tropical disease affecting approximately 200 million people worldwide. With the ultimate goal of understanding the molecular basis for neuromuscular transmission in these parasitic flatworms, we have previously cloned three transcripts from *Schistosoma mansoni* that code for one L-type-like and two non L-type high voltage-activated Ca_v channel α_1 subunits [13]. Heterologous expression of these α_1 subunits in *Xenopus* oocytes and mammalian cell lines has proved problematic, perhaps because of the relatively high A-T content of these coding regions, or the lack of a specific chaperone in these systems. Additionally, we have identified two Ca_v channel β subunits from schistosomes and other platyhelminths: a conventional β subunit ($SmCa_v\beta$), and a variant β subunit ($SmCa_v\beta_{var}$), which appears to be unique to platyhelminths and has unusual structural and functional features [14,15].

When heterologously expressed in *Xenopus* oocytes, the conventional schistosome $Ca_v\beta$ subunit significantly increases $Ca_v2.3$ current amplitude, and shifts the steady state inactivation curve to more hyperpolarized potentials [16] (in these experiments, we use the robustly expressing human $Ca_v2.3$ α_1 subunit as a "reporter" to assess β subunit function). The actions of this β subunit are consistent with those of mammalian $Ca_v\beta$ subunits [10]. Here, we have reproduced and extended our previous data on modulation of $Ca_v2.3$ currents by the schistosome $SmCa_v\beta$ subunit ($SmCa_v\beta$) in a mammalian cell system, which may better approximate the cellular milieu in which these channels are found *in situ*. *Xenopus* oocytes are widely used in expression of ion channels and other proteins, in part because they are primed for high levels of protein translation. However, most other cells are not that strongly geared towards this role. Oocytes are much larger than adult, differentiated cells and contain high amounts of yolk granules. In addition, the mammalian cell line HEK does not express the endogenous $Ca_v\beta$ subunit that complicates analysis of heterologously expressed Ca_v channels in *Xenopus* oocytes [17]. Finally, adult *S. mansoni* live in a mammalian host environment.

Interestingly, during these studies, we observed a rapid run-down of the currents produced by $Ca_v2.3$ channels

co-expressed with this schistosome $Ca_v\beta$ subunit. Decrease of Ca^{2+} channel activity under whole-cell patch-clamp, a configuration of the patch-clamp technique that disrupts the contact between membrane and cytoplasm, is a well-known phenomenon [18-21]. However, very few studies have dealt with the structural and biochemical causes for run-down, and those studies focus primarily on L-type Ca^{2+} channels. Notably, Kameyama and collaborators were able to relate run-down of L-type Ca^{2+} channels to the Ca^{2+}-binding protein calmodulin [22]. Here we investigate the mechanism of this β subunit-dependent rundown, examining the role of several forms of ATP and cations in run-down of the $Ca_v2.3/SmCa_v\beta$ complex. Additionally, we use a truncated β subunit protein to provide clues regarding the molecular substrate within the $SmCa_v\beta$ subunit that mediates run-down of $Ca_v2.3/SmCa_v\beta$ currents.

Results

SmCa_vβ modulates activation and inactivation of Ca_v2.3 in a conventional manner

To assess the modulatory phenotype of $Ca_v\beta$ subunits, a HEK-293 cell line stably expressing the human $Ca_v2.3d$ subunit (GB Acc. # <u>L27745</u>) was used. Using Ca^{2+} as the charge carrier, currents produced by $Ca_v2.3$ alone peaked at +30 mV with an average amplitude of -261 ± 20 pA (n = 15). Co-expression of $SmCa_v\beta$ increased peak amplitudes to -1640 ± 276 pA (n = 5) and shifted the I–V peak leftwards, to +20 mV (Figure 1A,B).

Using Ca^{2+} as the charge carrier, the decaying phase of $Ca_v2.3$ currents produced by $Ca_v2.3$ channels alone or with $SmCa_v\beta$ subunits was well fitted by a double exponential function with fast (τ_{fast}) and slow (τ_{slow}) time constants of inactivation (Table 1). The double exponential fit to the decay of currents produced by $Ca_v2.3$ in response to a pulse to +30 mV had a fast time constant of 16 ms that contributed 66% to total current decay, and a slow time constant of 69 ms that represented 34% of total current decay. The double exponential fit to the decay of currents produced by $Ca_v2.3$ co-expressed with $SmCa_v\beta$ in response to a depolarizing pulse to +20 mV had a fast time constant of 31 ms, which contributed 55% to total current decay, and a slow time constant of 116 ms that contributed 45% to total inactivation. Fundamentally, $SmCa_v\beta$ slowed macroscopic inactivation of $Ca_v2.3$ currents by increasing the time constants of both the fast and slow components while simultaneously decreasing the contribution of the fast component and increasing the contribution of the slow component to total inactivation (Figure 1C and Table 1). Co-expression of $SmCa_v\beta$ markedly shifted the midpoint of steady-state inactivation in the hyperpolarizing direction (Figure 1D). Midpoints of single order Boltzmann fits to steady-state inactivation curves of $Ca_v2.3$ and $Ca_v2.3$ + $SmCa_v\beta$ currents were, respectively, -8 mV and -49 mV (P < 0.05, Student t-test). The

Figure 1
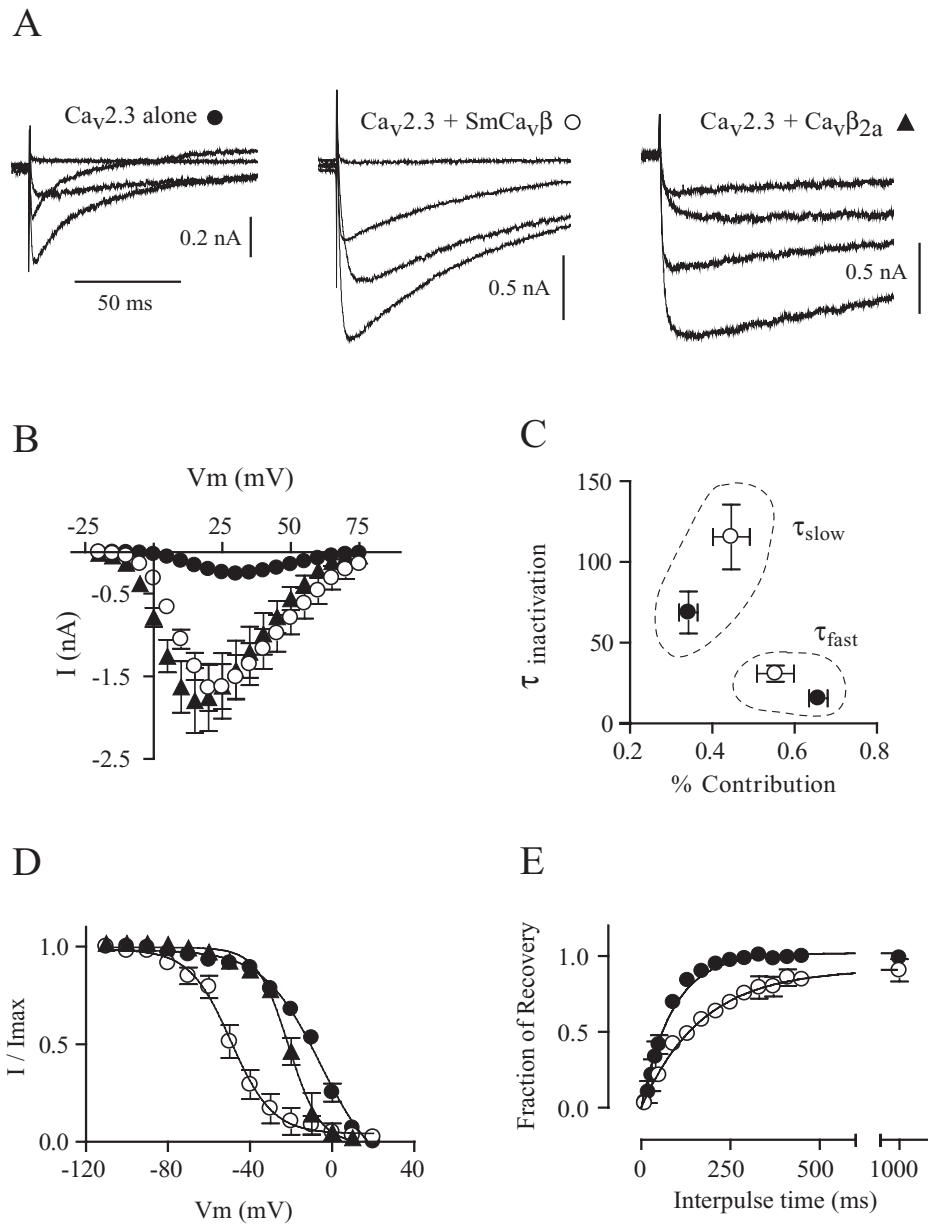**SmCa$_v$β modulates Ca$_v$2.3 currents in HEK cells**. *A*. Representative Ca^{2+} currents generated by voltage steps to -5, +15, +35 and +55 mV from a holding potential of -80 mV in HEK cells expressing Ca$_v$2.3 alone and in combination with SmCa$_v$β or Ca$_v$β$_{2a}$. *B*. Current-voltage relationships from HEK cells expressing Ca$_v$2.3 alone (filled circles) and in combination with SmCa$_v$β (open circles) or Ca$_v$β$_{2a}$ (filled triangles). Peak currents generated by voltage steps from -20 mV to +75 mV in 5 mV steps from a holding potential of -80 mV were measured. Data points represent mean ± s.e.m. N = 5–15. *C*. Two-variable plot showing the relationships between inactivation time constants and percentages of contribution to total inactivation for Ca$_v$2.3 alone (filled circles) and in combination with SmCa$_v$β (open circles). Data points represent mean ± s.e.m. N = 7–9. Slow time constants for the kinetic of recovery are grouped (dotted lines). Fast time constants of recovery from inactivation kinetics are also grouped (dotted lines). *D*. Voltage-dependence of inactivation (steady-state inactivation) for Ca$_v$2.3 alone (filled circles) and in combination with SmCa$_v$β (open circles) or Ca$_v$β$_{2a}$ (filled triangles). Lines represent fits to the Boltzmann function (see Materials and Methods); V$_{50}$ and slope values are shown in Table 1. Data points represent mean ± s.e.m. N = 3–6. *E*. Recovery from inactivation from -100 mV for Ca$_v$2.3 channels alone (filled circles) or in the presence of SmCa$_v$β (open circles), using Ba^{2+} as the charge carrier. Solid curves represent single exponential fits to the data. Values are means ± s.e.m. N = 3.

Table 1: SmCa$_v$β modulates inactivation of Ca$_v$2.3 currents

	Ca$_v$2.3 alone	Ca$_v$2.3 + SmCa$_v$β
Steady state inactivation		
V$_{50}$ (mV)	-8 ± 4 (3)	-49 ± 3 (3)*
Slope (mV/e-fold)	12 ± 2 (3)	10 ± 1 (3)
Macroscopic inactivation		
τ_{fast} (ms)	16 ± 3 (9)	31 ± 5 (7)*
% Contribution	66 ± 2%	55 ± 5%*
τ_{slow} (ms)	69 ± 13 (9)	116 ± 20 (7)
% Contribution	34 ± 2%	45 ± 5%*
Recovery from inactivation		
$\tau_{rec-80\ mV}$ (ms)	178 ± 28 (3)	252 ± 17 (4)
$\tau_{rec-100\ mV}$ (ms)	71 ± 7 (3)	168 ± 16 (3)*
$\tau_{rec-120\ mV}$ (ms)	38 ± 1 (3)	109 ± 10 (3)*

Data represent mean ± s.e.m. Number of repeats is indicated in parentheses. Asterisks indicate statistically significant difference (Student t test, P < 0.05).

slope factors of these Boltzmann fits to steady-state inactivation were not significantly different: 12 mV/e-fold for Ca$_v$2.3 and 10 mV/e-fold for Ca$_v$2.3 + SmCa$_v$β (Table 1).

SmCa$_v$β significantly slowed the rate of recovery from inactivation. The fractional recoveries of current as a function of time at -80, -100 and -120 mV were well fitted by a single exponential function with recovery time constants from inactivation (τ_{rec}). For example, τ_{rec} for Ca$_v$2.3 and Ca$_v$2.3 + SmCa$_v$β from -100 mV were, respectively, 71 and 168 ms (p < 0.05, Student t-test) (Figure 1E; see Table 1 for recovery time constants for the three potentials).

The mammalian (rat) β$_{2a}$ subunit (GB Acc. # M80545) increased current amplitude to a similar extent as the schistosome Ca$_v$β subunit, shifted the steady-state inactivation curve in the hyperpolarizing direction, although to a lesser degree than the schistosome Ca$_v$β subunit, slowed macroscopic inactivation, and shifted the I–V peak in the hyperpolarizing direction (Figure 1).

Ca$_v$2.3 currents run-down in the presence of SmCa$_v$β in a manner independent of Ca^{2+} but dependent on chelated forms of ATP and free Na$^+$

Currents produced by Ca$_v$2.3 progressively decrease in amplitude to approximately 75% of their initial values within ~2.5 minutes of establishing the whole-cell configuration, but only when SmCa$_v$β is co-expressed (Figure 2A). Over the same time frame, no run-down was observed for currents produced by Ca$_v$2.3 expressed alone, nor in the presence of the mammalian Ca$_v$β$_{2a}$ subunit nor with the structurally atypical schistosome SmCa$_v$β$_{var}$ subunit (Figure 2B). Substitution of CaCl$_2$ by an equimolar concentration of BaCl$_2$ did not prevent rundown, indicating that this phenomenon is Ca^{2+} independent (Figure 2A).

We hypothesized that this rapid run-down could be caused by physical dissociation between SmCa$_v$β and Ca$_v$2.3. However, as the kinetics of inactivation and the steady state inactivation properties were identical before and after run-down (Figure 2C,D), it seems likely that the association between Ca$_v$2.3 and SmCa$_v$β remained intact in these conditions.

Since Mg^{2+} is known to block Ca^{2+} channels from the intracellular side, we replaced Mg^{2+}-ATP with an equimolar concentration (5 mM) of Na$^+_2$-ATP, yet under these conditions we still observed significant run-down that, again, was dependent upon co-expression of the schistosome Ca$_v$β subunit (Figure 3A). No run-down was observed in whole-cell patch-clamp experiments using a "minimal" internal solution without ATP (Figure 3C). Further experiments indicate that non-chelated forms of ATP (Tris$_2$-ATP) do not mediate SmCa$_v$β-dependent Ca$_v$2.3 run-down (Figure 3B). Currents produced by Ca$_v$2.3/Ca$_v$β$_{2a}$ did not run-down in the presence of 5 mM intracellular NaCl, Na$_2$-ATP, Tris$_2$·ATP or in minimal intracellular solution (Figures 3D1 and 3D2).

Next we explored the possibility that this particular form of run-down was caused by the cations associated with the ATP molecule (Mg^{2+} and Na$^+$). Free Mg^{2+} reduced currents produced by Ca$_v$2.3 alone by about 75%, and by about 90% when SmCa$_v$β was co-expressed (Figure 4); therefore, since it would be very challenging to distinguish Ca^{2+} current decrease due to run-down from Ca^{2+} current decrease due to blockade by internal Mg^{2+}, we did not pursue rundown studies in the presence of free Mg^{2+}. However, in contrast with Mg^{2+}, free Na$^+$ did not suppress the activity of Ca$_v$2.3 channels expressed alone or co-expressed with the schistosome SmCa$_v$β or with the mammalian Ca$_v$β$_{2a}$ subunit (Figure 5A–D). However, substituting Mg^{2+}-ATP with NaCl resulted in significant run-down (Figure 5E), indicating Na$^+$-dependent modulation of channels containing SmCa$_v$β.

The structural basis for run-down mediated by SmCa$_v$β resides in its acidic N-terminal domain

The N-terminus of the SmCa$_v$β subunit contains an atypical domain that is rich in glutamic acid and aspartic acid residues (Figure 6A). Since BLAST screens for similar domains in other proteins did not yield any hits, we set to investigate whether this N-terminal domain represents the structural base for the atypical modulation of the SmCa$_v$β subunit. Furthermore, there is precedence for important modulatory effects on Ca$_v$ channels localizing to the N-terminal regions of β subunits [23-26]. To this end, we created a truncated version of SmCa$_v$β that lacks the first forty-six amino acids containing this acid-rich domain (Figure 6A), and tested whether it still caused Ca$_v$2.3 currents to run-down. The N-terminally truncated
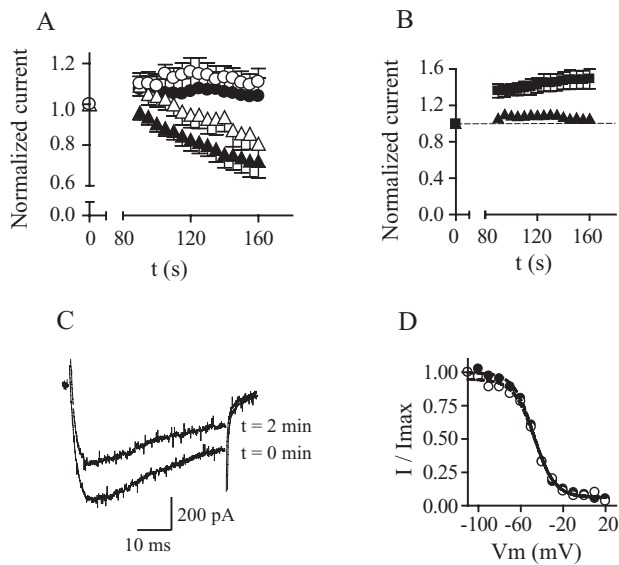
Figure 2
SmCa$_v$β-dependent run-down of Ca$_v$2.3 currents. *A*.
Relative peak amplitude of currents produced by Ca$_v$2.3
channels alone (circles) and in combination with SmCa$_v$β (tri-
angles), plotted as a function of time. Currents were normal-
ized with respect to those measured immediately after
rupturing the patch membrane (t = 0). Ca^{2+} currents (filled
symbols) and Ba^{2+} currents (open symbols) are shown. Data
points represent mean ± s.e.m. *B*. Relative amplitude of cur-
rents produced by Ca$_v$2.3 in combination with Ca$_v$β$_{2a}$
(squares) or SmCa$_v$β$_{var}$ (triangles), plotted as a function of
time. As in A, currents were normalized with respect of
those at time 0, measured immediately after break-in. Data
points represent mean ± s.e.m, N = 3 – 5. *C*. Ca^{2+} currents
generated by Ca$_v$2.3 in the presence of SmCa$_v$β at t = 0 min
and at t = 2 min. Note that the kinetics of macroscopic inac-
tivation remains unchanged. *D*. Voltage-dependence of inacti-
vation (steady-state inactivation) at t = 0 min (filled circles)
and at t = 2 min (open circles). Solid lines represent fits to
the Boltzmann function.

Figure 3
**Run-down of Ca$_v$2.3/SmCa$_v$β currents in the presence
of intracellular forms of ATP**. Relative current amplitude
of currents produced by Ca$_v$2.3 (filled circles) channels alone
and in combination with SmCa$_v$β (open circles) plotted as a
function of time in the presence of 5 mM Na$_2^+$-ATP in the
patch-pipette solution (A), 5 mM Tris$_2$-ATP (B), and using a
"minimal" pipette solution, with no ATP (C). Currents were
normalized with respect to those measured immediately
after rupturing the patch membrane (t = 0). Panels D1 and
D2 show current amplitude produced by Ca$_v$2.3/SmCa$_v$β$_{2a}$
channels as a function of time for all conditions explained
above. Symbols are as shown on the figure. Values are means
± s.e.m, N = 3 – 8.

SmCa$_v$β subunit enhanced Ca$_v$2.3 currents, slowed their
macroscopic inactivation and shifted their steady-state
inactivation to the same extent as the wild type SmCa$_v$β
subunit (Figure 6B,C). However, unlike the wild-type ver-
sion of SmCa$_v$β, the N-terminally truncated SmCa$_v$β sub-
unit did not induce run-down of Ca^{2+} currents within 2–3
minutes of establishing the whole-cell configuration with
an internal solution containing either 5 mM Mg^{2+}-ATP
(Figure 6D,F), or 5 mM NaCl (Figure 6E,F).

Discussion
In this study we set out to characterize the modulatory
phenotype of a Ca$_v$β subunit from the parasitic trematode
S. mansoni. This β subunit is phylogenetically close to
other Ca$_v$β subunits [14]. The mammalian HEK-293 cell
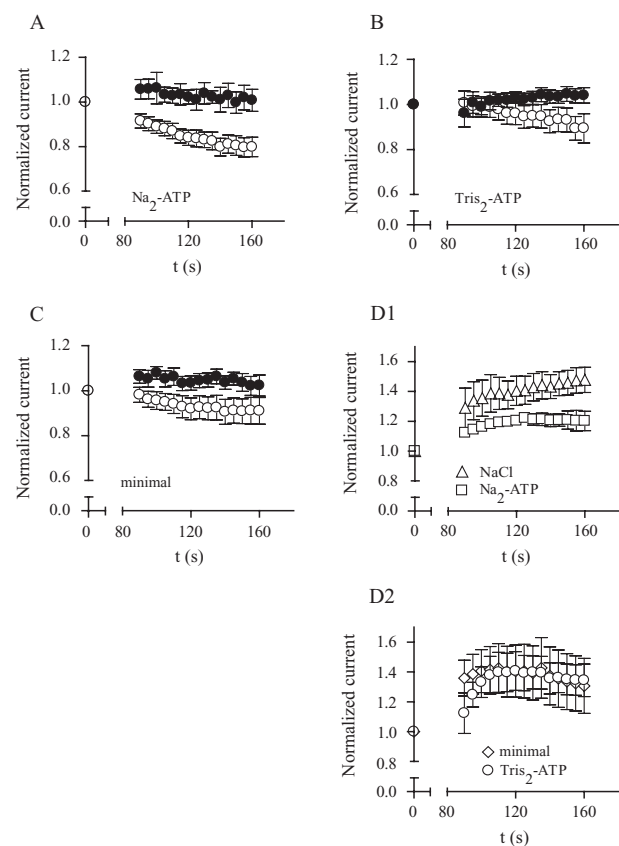line was used as the expression system and the mamma-

lian Ca$_v$2.3 channel splice variant "d" as our "test" α$_1$ sub-
unit. This splice variant is susceptible to modulation by
Ca$_v$β subunits [27] and is the longest of all known ver-
sions of the Ca$_v$2.3 subunit [28]. Our data show that
SmCa$_v$β exhibits similar modulatory phenotypes in HEK
cells and *Xenopus* oocytes. Additionally, SmCa$_v$β slows
recovery from inactivation of Ca$_v$2.3 currents using Ba^{2+} as
the charge carrier, i.e. in the absence of intracellular Ca^{2+}
accumulation. Using strontium as the charge carrier,
mammalian and jellyfish Ca$_v$β subunits also slow recov-
ery from inactivation of this same channel in conditions
in which Ca^{2+} does not accumulate in the intracellular

compartment [11]. However, it is important to note that recovery from inactivation appears to depend heavily on the identity of the $Ca_v\alpha_1$ subunit being assayed: all jellyfish and mammalian $Ca_v\beta$ subunits delayed recovery from inactivation of $Ca_v2.3$ channels, but accelerated the recovery of the jellyfish L-type Ca_v channel [11].

SmCa$_v\beta$-dependent run-down of Ca$_v$2.3 currents
While characterizing the modulatory phenotype of SmCa$_v\beta$, we consistently observed a rapid run-down of $Ca_v2.3$ currents only in the presence of SmCa$_v\beta$. This contrasts with previous studies, in which run-down appears to occur in the α_1 subunit, independently of accessory subunits [29-31]. Down-regulation of Ca^{2+} currents caused by interaction of $Ca_v\beta$ subunits with intracellular proteins is well documented. For example, interaction of $Ca_v\beta$ subunits with small GTPases of the RGK family [32], with large GTPases of the dynamin family [33], or with the nuclear protein HP1 [34] results in down-regulation of Ca^{2+} currents. Our data represent the first case, to our knowledge, of down-regulation of Ca^{2+} currents by interactions between $Ca_v\beta$ subunits and chelated forms of ATP or Na^+ ions, which are likely relevant to platyhelminth physiology. Unlike previous studies, in which hydrolysable forms of ATP suppress Ca^{2+} current run-down [35,36], here we show that two physiologically relevant, hydrolysable forms of ATP induce SmCa$_v\beta$-mediated decrease in $Ca_v2.3$ activity. The possibility that run-down was caused by Mg^{2+} ions that dissociate from the ATP molecule was considered, but the fact that free Mg^{2+} dramatically suppressed $Ca_v2.3$ currents posed a significant challenge to explore this possibility. These results are reminiscent of the effects of Mg^{2+} ions at a similar concentration on L-type Ca_v channels, which occurs by their binding to a low-affinity site at the pore of the $\alpha 1$ subunit [37]. Since ATP associates with Na^+ ions under physiological conditions [38], we also measured run-down of $Ca_v2.3/SmCa_v\beta$ channels in the presence of intracellular Na^+_2-ATP. Because we detected significant run-down under these conditions, and knowing that the binding constant between Na^+ ions and ATP is relatively low, about 13 M^{-1} (in contrast to 9000 M^{-1} for Mg^{2+}, [39]), we hypothesized that Na^+ ions that had dissociated from ATP were causing this run-down. Experiments using NaCl instead of Na^+_2-ATP confirmed this hypothesis.

Our study is not the first to show $Ca_v\beta$-dependent run-down of non-L type Ca^{2+} current. The mammalian $Ca_v\beta$ subunit appears to enhance run-down of the non-L-type, $Ca_v2.1 \alpha_1$ subunit [40]. However, it is important to note that in that study, run-down occurred under the two-electrode voltage clamp configuration on *Xenopus* oocytes, where the connection between cytoplasm and plasma membrane remains largely intact. Therefore the mechanism(s) of run-down employed by the mammalian $Ca_v\beta$

subunit is likely to be distinct from that used by the schistosome $Ca_v\beta$ subunit.

Molecular substrate for SmCa$_v\beta$-dependent Mg^{2+}-ATP and Na$^+$ sensitivity
Since the conventional SmCa$_v\beta$ subunit contains a string of acidic residues in the N-terminal domain that is not found in its mammalian counterparts, we generated a version of this subunit that lacked this region, to test whether this unique domain is the molecular substrate for this particular form of run-down. Deletion of this acidic, N-terminal fragment did not change the modulatory phenotype of SmCa$_v\beta$ on current amplitude, inactivation kinetics or steady-state inactivation. However, in contrast to our results with wild type SmCa$_v\beta$, $Ca_v2.3$ currents did not run down when co-expressed with this mutated subunit, using Ca^{2+} as the charge carrier and in the presence of intracellular free Na^+ or Mg^{2+}-ATP. It seems likely that sensitivity to intracellular Mg^{2+}-ATP and free Na^+ resides in all or part of the string of acidic residues of the SmCa$_v\beta$ subunit.

Physiological relevance
Several reports have shown that the Ca^{2+} currents of platyhelminth muscle and nerve cells are very labile, running down within minutes or even seconds after establishing the whole-cell patch-clamp configuration. In previous work, the intracellular solution used to record voltage-gated Ca^{2+} currents from muscle cells of *S. mansoni* was titrated with NaOH to bring the pH to a physiological value [41]. We have empirically calculated that this action would bring the concentration of Na^+ to approximately 19 mM, which is sufficient to reduce Ca^{2+} currents modulated by SmCa$_v\beta$ significantly, according to our data. Similarly, Ca^{2+} currents recorded from isolated muscle cells of the free-living flatworm *Bdelloura candida* run-down within 20 seconds of establishing the whole-cell configuration [42]: It is tempting to speculate that this run-down was caused by the relatively high concentration of NaCl (30 mM) added to the intracellular solution in these experiments.

Our previous studies have identified a different schistosome $Ca_v\beta$ subunit (SmCa$_v\beta_{var}$; [14]), which does not exhibit the hallmark action of $Ca_v\beta$ subunits, namely, to increase Ca^{2+} current density. Together with the data presented here, this raises the question of whether schistosomes employ unique strategies to modulate excitability via atypical modulation of HVA Ca_v channels, information that could be useful in the design of targeted therapies to treat schistosomiasis.

Conclusion
We have identified novel functions for a schistosome $Ca_v\beta$ subunit, namely to confer Ca^{2+} currents with sensitivity to intracellular Mg^{2+}-ATP and Na^+ ions, which translates into a reduced ability on the part of this $Ca_v\beta$ subunit to
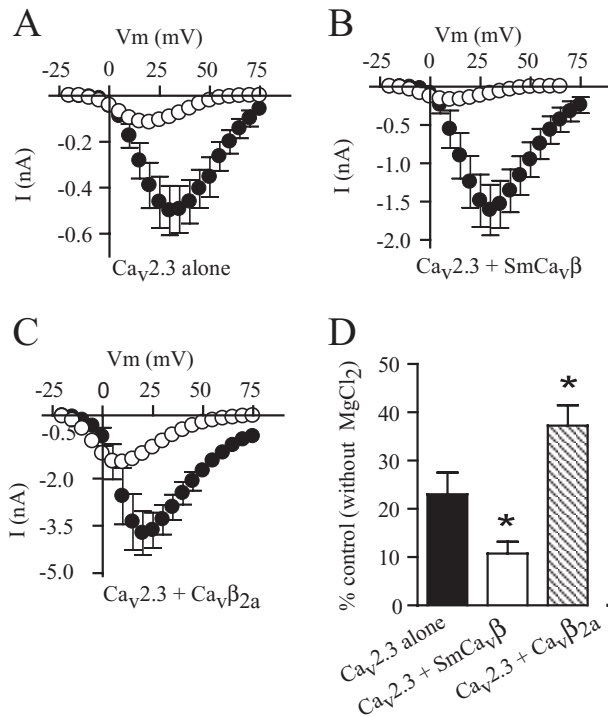
Figure 4
Mg^{2+} block of $Ca_v2.3$ channels expressed alone and co-expressed with $SmCa_v\beta$ or $Ca_v\beta_{2a}$. Current-voltage relationships from HEK cells expressing $Ca_v2.3$ subunits alone (A), co-expressing $Ca_v2.3$ and $SmCa_v\beta$ subunits (B) or co-expressing $Ca_v2.3$ and $Ca_v\beta_{2a}$ subunits (C) in minimal intracellular solution (filled circles) and in intracellular solution containing 5 mM $MgCl_2$ (open circles). Peak currents generated by voltage steps from -20 mV to +75 mV in 5 mV steps from a holding potential of -80 mV are plotted. Data points represent mean ± s.e.m. *D*. Peak current amplitude in the presence of 5 mM internal $MgCl_2$ relative to peak current amplitude in the absence of $MgCl_2$ for $Ca_v2.3$ subunits alone, co-expressed with $SmCa_v\beta$ subunits or co-expressed with $Ca_v\beta_{2a}$ subunits. Asterisks denote statistically significant difference with respect to Mg^{2+} block of $Ca_v2.3$ channels alone ($p < 0.05$), N = 5 – 7.

increase Ca^{2+} currents. We conclude that the molecular basis for this atypical sensitivity to both Mg^{2+}-ATP and Na^+ ions resides in a domain or domains located within the first forty-six amino acids of $SmCa_v\beta$, which contains a string of twenty-two aspartic and glutamic acid residues not present in other $Ca_v\beta$ subunits.

Methods
Materials
Tissue culture dishes were purchased from Corning (NY, USA), Dulbecco's modified Eagle's media (DMEM) was purchased from Invitrogen, poly-L-lysine and ATP salts were purchased from Sigma. The transfection reagent, Tfx,

was purchased from Promega. Restriction enzymes were from NEB, and oligonucleotide primers were from MWG Biotech.

Preparation of eukaryotic expression plasmids encoding $SmCa_v\beta$
Using standard methods, we cloned all $Ca_v\beta$ subunits into the pXOOM vector [43], which is optimized for expression of inserts in mammalian cells (under control of a cytomegalovirus promoter), and contains the gene for green fluorescent protein (GFP) as a marker for transfection. For $SmCa_v\beta$, the insert from the original $SmCa_v\beta$ clone in pCR4-TOPO (Invitrogen) was amplified using Phusion high-fidelity DNA polymerase (NEB). Primers were designed against the beginning and end of the coding regions of the sequence, and included appropriate restriction sites for insertion into pXOOM. The primers were: Forward: 5'-GGAAGCTTATGGCTGGTGATCGAG-GATATTCA-3', which includes two G residues and a *Hind III* site at the 5' end; and Reverse: 5'-GGGCGGCCGCT-TAAATCATGATTGAACCTTGACGA-3', which includes two G residues and a *Not I* site at the 5' end. Following an initial 98° denaturation for 30 seconds and 25 cycles of 98° for 10 s, 68° for 30 s, and 72° for 2 min, the reaction was purified over a QiaQuick spin column (Qiagen), and digested with *Hind III* and *Not I*. The digested band was gel-purified using Quantum Prep Freeze-n-Squeeze columns (BioRad), Pellet Paint (Novagen) was added as carrier, and the product was ethanol-precipitated and ligated to pXOOM that had been digested with *Hind III* and *Not I* and gel-purified. All constructs were sequenced to verify the absence of PCR errors.

Cell culture and transfection of HEK293-$Ca_v2.3$ cells
HEK293 cells stably transfected with $Ca_v2.3d$ [44] were cultured in DMEM supplemented with L-glutamine, glucose and 10% foetal bovine serum in a humidified atmosphere (95%) at 5% CO_2 and 37°C. Cells were used for up to 20 passages and were split every 2–4 days. For electrophysiological recordings, cells were seeded in Petri dishes coated with poly-l-lysine, and transfection of auxiliary β subunits was performed with Tfx on cells at a confluence of 50–60%, using 1 μg of the construct and a DNA: Tfx ratio of 1:2. Cells exhibiting green fluorescence were used for further study.

Construction of a N-terminal deletion mutant of the $SmCa_v\beta$ subunit
To generate a mutant subunit lacking amino acids 2–46 of the N terminus domain, a diluted sample of the $SmCa_v\beta$ clone was used as template for amplification of the truncated insert by PCR. The forward primer (5'-GGGGATC-CATGGAAAATGCTCGTCAGGGAACGG-3') was designed to bind to the $SmCa_v\beta$ clone, starting from nucleotide 142. This forward primer contains a start codon, a Kozak
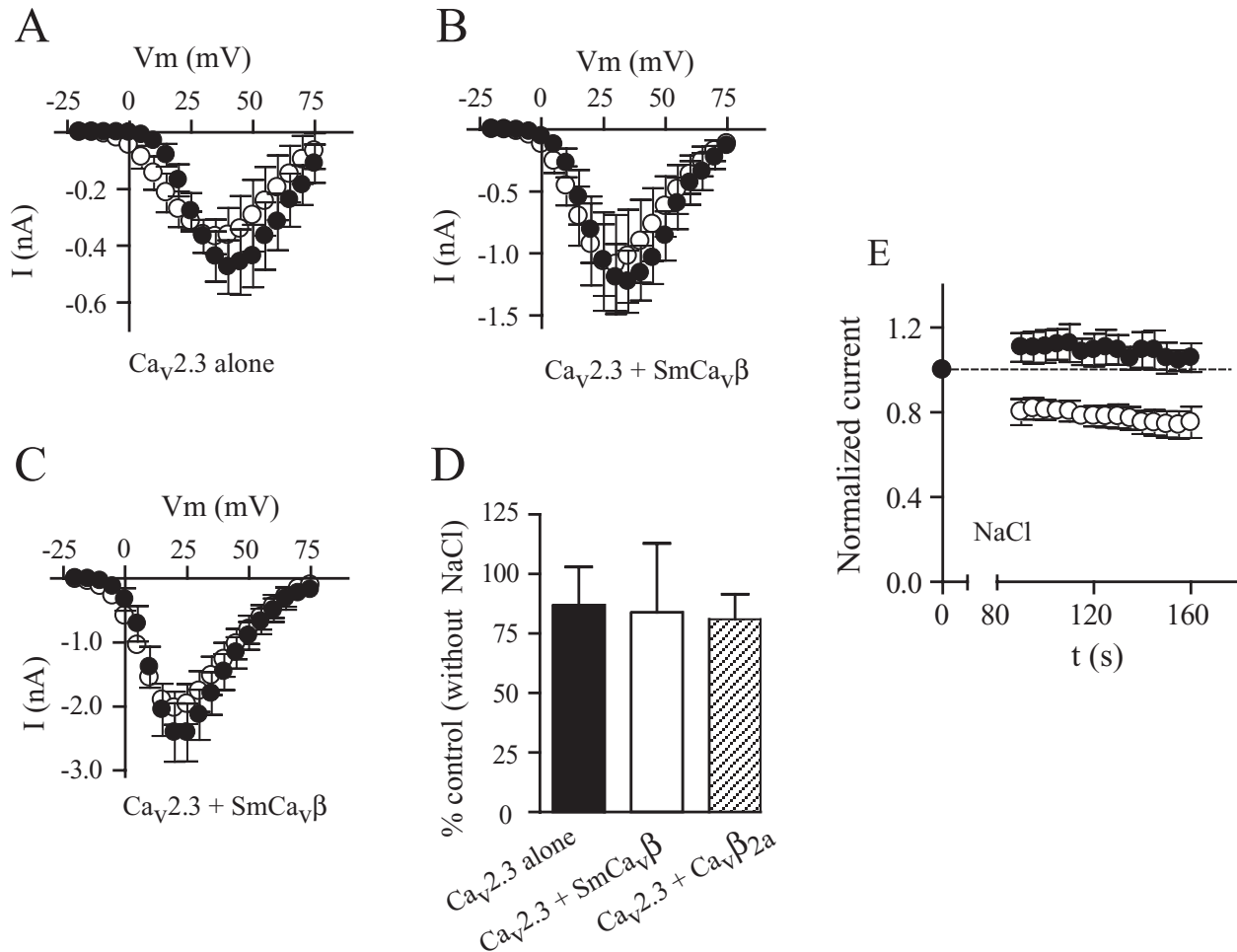
Figure 5
Intracellular free Na+ does not block Ca$_v$2.3 channels expressed alone or co-expressed with SmCa$_v$β or Ca$_v$β$_{2a}$ but induces SmCa$_v$β-dependent run-down of Ca$_v$2.3 currents. Current-voltage relationships from HEK cells expressing Ca$_v$2.3 subunits alone (A), co-expressing Ca$_v$2.3 and SmCa$_v$β subunits (B) or co-expressing Ca$_v$2.3 and Ca$_v$β$_{2a}$ subunits (C) in minimal intracellular solution (filled circles) and in intracellular solution containing 5 mM NaCl (open circles). Peak currents generated by voltage steps from -20 mV to +75 mV in 5 mV steps from a holding potential of -80 mV are plotted. Data points represent mean ± s.e.m. (D) Peak current amplitude in the presence of 5 mM internal NaCl relative to peak current amplitude in the absence of NaCl for Ca$_v$2.3 subunits alone, co-expressed with SmCa$_v$β subunits or co-expressed with Ca$_v$β$_{2a}$ subunits. (E) Relative current amplitude of currents produced by Ca$_v$2.3 (filled circles) channels alone and in combination with SmCa$_v$β (open circles) plotted as a function of time in the presence of 5 mM NaCl in the patch-pipette solution. Values are means ± s.e.m, N = 3 – 9.

sequence and a BamHI restriction site. The reverse primer was the same one used to amplify the full-length sequence. These PCR products were inserted into pXOOM and transformed into *E. coli*. Clones were sequenced to verify the deletion and to detect possible PCR errors.

Electrophysiology
Whole-cell recordings were obtained at room temperature 24 hours following transfection using an Axopatch 200B

(Molecular Devices). Cell capacitance was 12–25 pF. Series resistance was compensated by 70%. Voltage pulses from -20 mV to +70 mV were delivered in 5 mV increments from a holding potential of -80 mV. Data were acquired at sampling intervals of 50 μs and filtered at 5 kHz during acquisition. The pipette solution contained (mM): cesium methane sulfonate (110), HEPES (10), EGTA (9), Mg^{2+}-ATP (5); pH (CsOH) 7.3, with variations, as noted. The bath solution contained (mM): CaCl$_2$ (10),
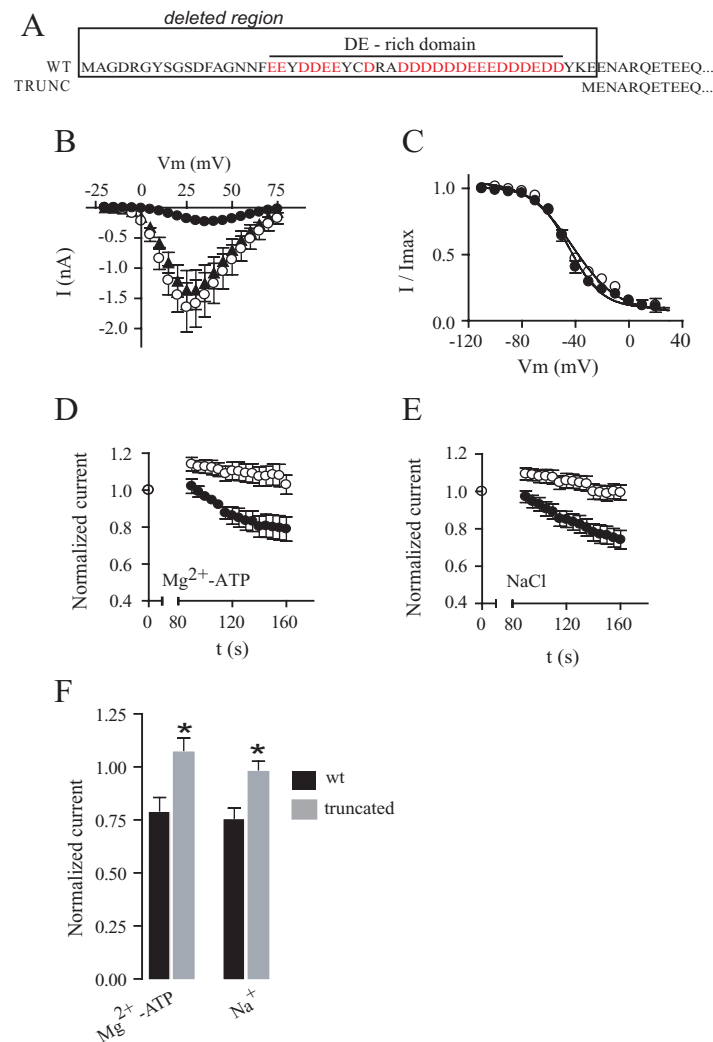
Figure 6
The N-terminal domain of SmCa$_v$β is the molecular substrate for Na$^+$ and Mg^{2+}-ATP mediated block of Ca$_v$2.3 currents. *A*. Diagram showing the portion of the N-terminal domain, including a domain rich in aspartic acid and glutamic acid (DE-rich domain), that is removed by the truncation. Acidic residues are in red. *B*. Current-voltage relationships from HEK cells expressing Ca$_v$2.3 alone (filled circles) and in combination with SmCa$_v$β (open circles) or N-terminally truncated SmCa$_v$β (filled triangles). Peak currents generated by voltage steps from -20 mV to +75 mV in 5 mV steps from a holding potential of -80 mV were measured. Data points represent mean ± s.e.m. N = 6–7. *C*. Voltage-dependence of inactivation (steady-state inactivation) for Ca$_v$2.3 alone co-expressed with SmCa$_v$β (filled circles) or with its N-terminally truncated version (open circles). Lines represent fits to the Boltzmann function. *D*. Relative peak current amplitude of currents produced by Ca$_v$2.3 channels in the presence of internal 5 mM Mg^{2+}-ATP co-expressed with the wild type SmCa$_v$β subunit (filled circles) or with the N-terminally truncated SmCa$_v$β subunit (open circles) plotted as a function of time. Currents were normalized with respect to those measured immediately after rupturing the patch membrane (t = 0). Data points represent mean ± s.e.m. N = 5. *E*. Relative current amplitude of currents produced by Ca$_v$2.3 channels in the presence of internal 5 mM NaCl co-expressed with the wild type SmCa$_v$β subunit (filled circles) or with the N-terminally truncated SmCa$_v$β subunit (open circles) plotted as a function of time. Currents were normalized with respect to those measured immediately after rupturing the patch membrane (t = 0). Data points represent mean ± s.e.m. N = 10–13. *F*. Comparison between the relative current amplitudes produced by Ca$_v$2.3 channels co-expressed with SmCa$_v$β (in black) or with its N-terminally truncated version (in grey), in the presence of intracellular 5 mM Mg^{2+}-ATP (left), or in the presence of 5 mM NaCl (right), after 2.5 minutes of establishing the whole-cell configuration. Asterisks denote statistical difference with respect to current amplitude for Ca$_v$2.3 co-expressed with wild type SmCa$_v$β (Student t test, p < 0.05).

TEA-Cl (160), HEPES (10), EGTA (0.1); pH (TEA-OH) 7.4. Patch pipettes were pulled from borosilicate glass and fire polished before each experiment. To ensure a fast dialysis of the intracellular compartment, only pipettes with resistances between 0.8 and 1.2 MΩ were used. Membrane seals were obtained by applying negative pressure. All experiments were performed at room temperature (22°C). The voltage-dependence of steady state inactivation was determined by measuring the peak current evoked with a depolarising pulse to elicit the maximum current as a function of the voltage of a preceding 1.5 s pre-pulse test (between -110 and +20 mV). Steady-state inactivation curves were fitted by a sigmoid (Boltzmann) distribution of the form:

$$F (V) = I_{max}/\{1 + \exp [V_{0.5} - V)/K]\}$$

Where I_{max} is the maximal current, V is the pre-pulse voltage, K is the slope factor and $V_{0.5}$ is the voltage at which inactivation is half-maximal.

To study inactivation as a function of time, the decaying phases of the inward currents evoked by a test pulse to +20 or +30 mV were fitted to a double exponential equation of the form: $I (t) = I_0 + I_1 \exp (-t/\tau_1) + I_2 \exp (-t/\tau_2)$, where τ_1 and τ_2 represent the fast and the slow time constants of inactivation, respectively, I_1 and I_2 represent the relative contribution of each component to inactivation and I_0 is the offset. To assess the rate of recovery from inactivation from the closed state, a two-pulse protocol was used. Two test pulses to +20 or +30 mV were separated by a recovery step to -80, -100 or -120 mV for varying amounts of time (from 10 ms to 1 second). The length and voltage of the first test pulse was adjusted accordingly for each particular channel combination. For example, currents produced by Ca$_v$2.3 channels alone were maximal at approximately +30 mV and inactivated completely within 100 ms, whereas currents produced by Ca$_v$2.3/SmCa$_v\beta$ were maximal at approximately +20 mV and required several seconds to inactivate fully. In the latter case, recovery from inactivation was measured using Ba^{2+} instead of Ca^{2+} as the charge carrier (Ba^{2+} currents inactivate faster than Ca^{2+} currents produced by Ca$_v$2.3 [45]), thereby decreasing the need to use an excessively long depolarising first pulse protocol, which could compromise cell viability. The currents evoked by the second pulse of this double-pulse protocol were normalized to the currents produced by the first pulse and plotted against the duration of the inter-pulse interval.

Statistical analyses
Statistical comparisons were carried out using the Student t-test. Data are presented as means ± s.e.m. Number of repeats is indicated in parentheses.

Authors' contributions
VSR carried out the molecular and electrophysiological studies, made substantial contributions to conception and experimental design, and drafted the manuscript. TS provided the HEK cell line stably transfected with Ca$_v$2.3 and made a significant contribution to the interpretation of the data. RMG carried out molecular work and contributed to experimental design as well as to the writing of the manuscript. All authors read and approved the final manuscript.

Acknowledgements

References
1. Fabiato A, Fabiato F: **Calcium and cardiac excitation-contraction coupling.** *Annu Rev Physiol* 1979, **41**:473-484.
2. Hirano K: **Current topics in the regulatory mechanism underlying the Ca²⁺ sensitization of the contractile apparatus in vascular smooth muscle.** *J Pharmacol Sci* 2007, **104**:109-115.
3. West AE, Chen WG, Dalva MB, *et al.*: **Calcium regulation of neuronal gene expression.** *Proc Natl Acad Sci USA* 2001, **98**:11024-11031.
4. Uchitel OD, Protti DA, Sanchez V, Cherksey BD, Sugimori M, Llinas R: **P-type voltage-dependent calcium channel mediates presynaptic calcium influx and transmitter release in mammalian synapses.** *Proc Natl Acad Sci USA* 1992, **89**:3330-3333.
5. Evans RM, Zamponi GW: **Presynaptic Ca²⁺ channels – integration centers for neuronal signaling pathways.** *Trends Neurosci* 2006, **29**:617-624.
6. Yu FH, Yarov-Yarovoy V, Gutman GA, Catterall WA: **Overview of molecular relationships in the voltage-gated ion channel superfamily.** *Pharmacol Rev* 2005, **57**:387-395.
7. Catterall WA: **Structure and regulation of voltage-gated Ca²⁺ channels.** *Annu Rev Cell Dev Biol* 2000, **16**:521-555.
8. Brice NL, Berrow NS, Campbell V, Page KM, Brickley K, Tedder I, Dolphin AC: **Importance of the different beta subunits in the membrane expression of the alpha1A and alpha2 calcium channel subunits: studies using a depolarization-sensitive alpha1A antibody.** *Eur J Neurosci* 1997, **9**:749-759.
9. Singer D, Biel M, Lotan I, Flockerzi V, Hofmann F, Dascal N: **The roles of the subunits in the function of the calcium channel.** *Science* 1991, **253**:1553-1557.
10. Dolphin AC: **Beta subunits of voltage-gated calcium channels.** *J Bioenerg Biomembr* 2003, **35**:599-620.
11. Jeziorski MC, Greenberg RM, Anderson PA: **Calcium channel beta subunits differentially modulate recovery of the channel from inactivation.** *FEBS Lett* 2000, **483**:125-130.
12. Takahashi SX, Mittman S, Colecraft HM: **Distinctive modulatory effects of five human auxiliary beta2 subunit splice variants on L-type calcium channel gating.** *Biophys J* 2003, **84**:3007-3021.
13. Kohn AB, Lea J, Roberts-Misterly JM, Anderson PA, Greenberg RM: **Structure of three high voltage-activated calcium channel alpha1 subunits from Schistosoma mansoni.** *Parasitology* 2001, **123**:489-497.
14. Kohn AB, Anderson PA, Roberts-Misterly JM, Greenberg RM: **Schistosome calcium channel beta subunits. Unusual modulatory effects and potential role in the action of the antischistosomal drug praziquantel.** *J Biol Chem* 2001, **276**:36873-36876.
15. Jeziorski MC, Greenberg RM: **Voltage-gated calcium channel subunits from platyhelminths: potential role in praziquantel action.** *Int J Parasitol* 2006, **36**:625-632.
16. Kohn AB, Roberts-Misterly JM, Anderson PA, Greenberg RM: **Creation by mutagenesis of a mammalian Ca²⁺ channel beta sub-

unit that confers praziquantel sensitivity to a mammalian Ca²⁺ channel.** *Int J Parasitol* 2003, **33**:1303-1308.

17. Tareilus E, Roux M, Qin N, Qin N, Olcese R, Zhou J, Stefani E, Birnbaumer L: **A Xenopus oocyte beta subunit: evidence for a role in the assembly/expression of voltage-gated calcium channels that is separate from its role as a regulatory subunit.** *Proc Natl Acad Sci USA* 1997, **94**:1703-1708.

18. Cavalie A, Ochi R, Pelzer D, Trautwein W: **Elementary currents through Ca²⁺ channels in guinea pig myocytes.** *Pflugers Arch* 1983, **398**:284-297.

19. Hagiwara S, Byerly L: **Calcium channel.** *Annu Rev Neurosci* 1981, **4**:69-125.

20. Kostyuk PG: **Intracellular perfusion of nerve cells and its effects on membrane currents.** *Physiol Rev* 1984, **64**:435-454.

21. McDonald TF, Pelzer S, Trautwein W, Pelzer DJ: **Regulation and modulation of calcium channels in cardiac, skeletal, and smooth muscle cells.** *Physiol Rev* 1994, **74**:365-507.

22. Xu JJ, Hao LY, Kameyama A, Kameyama M: **Calmodulin reverses rundown of L-type Ca²⁺ channels in guinea pig ventricular myocytes.** *Am J Physiol Cell Physiol* 2004, **287**:C1717-24.

23. Olcese R, Qin N, Schneider T, Neely A, Wei X, Stefani E, Birnbaumer L: **The amino terminus of a calcium channel β subunit sets rates of channel inactivation independently of the subunit's effect on activation.** *Neuron* 1994, **13**:1433-1438.

24. Takahashi SX, Mittman S, Colecraft HM: **Distinctive modulatory effects of five human auxiliary β2 subunit splice variants on L-type calcium channel gating.** *Biophys J* 84:3007-3021.

25. Harry JB, Kobrinsky E, Abernethy DR, Soldatov NM: **New short splice variants of the human cardiac Ca_vβ2 subunit: redefining the major functional motifs implemented in modulation of the Ca_v1.2 channel.** *J Biol Chem* 2004, **279**:46367-46372.

26. Vendel AC, Terry MD, Striegel AR, Iverson NM, Leuranguer V, Rithner CD, Lyons BA, Pickard GE, Tobet SA, Horne WA: **Alternative splicing of the voltage-gated Ca²⁺ channel β4 subunit creates a uniquely folded N-terminal protein binding domain with cell-specific expression in the cerebellar cortex.** *J Neurosci* 2006, **26**:2635-2644.

27. Jones LP, Wei SK, Yue DT: **Mechanism of auxiliary subunit modulation of neuronal alpha1E calcium channels.** *J Gen Physiol* 1998, **112**:125-143.

28. Pereverzev A, Leroy J, Krieger A, Malécot CO, Hescheler J, Pfitzer G, Klöckner U, Schneider T: **Alternate splicing in the cytosolic II–III loop and the carboxy terminus of human E-type voltage-gated Ca²⁺ channels: electrophysiological characterization of isoforms.** *Mol Cell Neurosci* 2002, **21**:352-365.

29. Hao LY, Kameyama A, Kuroki S, Nishimura S, Kameyama M: **Rundown of L-type Ca²⁺ channels occurs on the alpha 1 subunit.** *Biochem Biophys Res Commun* 1998, **247**:844-850.

30. Zhen XG, Xie C, Yamada Y, Zhang Y, Doyle C, Yang J: **A single amino acid mutation attenuates rundown of voltage-gated calcium channels.** *FEBS Lett* 2006, **580**:5733-5738.

31. Kepplinger KJ, Förstner G, Kahr H, Leitner K, Pammer P, Groschner K, Soldatov NM, Romanin C: **Molecular determinant for rundown of L-type Ca²⁺ channels localized in the carboxyl terminus of the 1C subunit.** *J Physiol* 2000, **529(Pt 1)**:119-130.

32. Beguin P, Nagashima K, Gonoi T, Shibasaki T, Takahashi K, Kashima Y, Ozaki N, Geering K, Iwanaga T, Seino S: **Regulation of Ca²⁺ channel expression at the cell surface by the small G-protein kir/Gem.** *Nature* 2001, **411**:701-706.

33. Gonzalez-Gutierrez G, Miranda-Laferte E, Neely A, Hidalgo P: **The Src homology 3 domain of the beta-subunit of voltage-gated calcium channels promotes endocytosis via dynamin interaction.** *J Biol Chem* 2007, **282**:2156-2162.

34. Hibino H, Pironkova R, Onwumere O, Rousset M, Charnet P, Hudspeth AJ, Lesage F: **Direct interaction with a nuclear protein and regulation of gene silencing by a variant of the Ca²⁺-channel beta 4 subunit.** *Proc Natl Acad Sci USA* 2003, **100**:307-312.

35. Yazawa K, Kameyama A, Yasui K, Li JM, Kameyama M: **ATP regulates cardiac Ca²⁺ channel activity via a mechanism independent of protein phosphorylation.** *Pflugers Arch* 1997, **433**:557-562.

36. Elhamdani A, Bossu JL, Feltz A: **ADP exerts a protective effect against rundown of the Ca²⁺ current in bovine chromaffin cells.** *Pflugers Arch* 1995, **430**:401-409.

37. Kuo CC, Hess P: **Block of the L-type Ca²⁺ channel pore by external and internal Mg²⁺ in rat phaeochromocytoma cells.** *J Physiol* 1993, **466**:683-706.

38. Melchior NC: **Sodium and potassium complexes of adenosinetriphosphate: equilibrium studies.** *J Biol Chem* 1954, **208**:615-627.

39. Wilson JE, Chin A: **Chelation of divalent cations by ATP, studied by titration calorimetry.** *Anal Biochem* 1991, **193**:16-19.

40. De Waard M, Campbell KP: **Subunit regulation of the neuronal alpha 1A Ca2+ channel expressed in Xenopus oocytes.** *J Physiol* 1995, **485(Pt 3)**:619-634.

41. Cobbett P, Day TA: **Functional voltage-gated Ca²⁺ channels in muscle fibers of the platyhelminth *Dugesia tigrina*.** *Comp Biochem Physiol A Mol Integr Physiol* 2003, **134**:593-605.

42. Blair KL, Anderson PAV: **Physiological and pharmacological properties of muscle cells isolated from the flatworm *Bdelloura candida* (Tricladia).** *Parasitology* 1994, **109**:325-335.

43. Jespersen T, Grunnet M, Angelo K, Klaerke DA, Olesen SP: **Dual-function vector for protein expression in both mammalian cells and *Xenopus laevis* oocytes.** *BioTechniques* 2002, **32**:536-8. 540.

44. Mehrke G, Pereverzev A, Grabsch H, Hescheler J, Schneider T: **Receptor-mediated modulation of recombinant neuronal class E calcium channels.** *FEBS Lett* 1997, **408**:261-270.

45. Leroy J, Pereverzev A, Vajna R, Qin N, Pfitzer G, Hescheler J, Malécot CO, Schneider T, Klöckner U: **Ca²⁺-sensitive regulation of E-type Ca²⁺ channel activity depends on an arginine-rich region in the cytosolic II–III loop.** *Eur J Neurosci* 2003, **18**:841-844.